buildings

MDPI

Article

Experimental Procedures of Accelerated Aging and Evaluation of Effectiveness of Nanostructured Products for the Protection of Volterra (Italy) Panchina Stone

Federica Fernandez [1,*], Silvia Germinario [2], Roberta Montagno [3], Roberta Basile [3], Leonardo Borgioli [4] and Rocco Laviano [2]

[1] Department of Architecture, University of Palermo, 90128 Palermo, Italy
[2] Department of Earth and Geoenvironmental Sciences, University of Bari Aldo Moro, 70125 Bari, Italy
[3] I.E.ME.S.T. Euro Mediterranean Institute of Science and Technology, 90139 Palermo, Italy
[4] C.T.S. SrL., Via Piave 20/22, 36077 Altavilla Vicentina, Italy
* Correspondence: federica.fernandez@unipa.it

Abstract: The aims of the research were to evaluate the effectiveness of the application of nanostructured products on Volterra calcarenite stone and to define the experimental conditions and procedures of accelerated aging tests, able to simulate different degradation on the studied lithotype. The work focused on methods of performing accelerated aging tests in order to simulate different effects of environmental decay involving stone used on a historical site. The rock samples were examined before and after three treatment types: cyclic salt spray chamber, cycles of freezing–thawing and cycles of thermal shock. After each artificial aging cycle, changes in appearance were noted and chemical and physical properties were measured so that the differences between untreated and treated samples could be compared. After applying nanostructured products on the sample surfaces, and assessing the effects of the accelerated aging, the protective performance of the coatings was evaluated using the contact angle test to evaluate the surface hygroscopicity. Moreover, scanning electron microscope (SEM-EDS) analysis was performed before and after each application of nanostructured coating to evaluate changes in the surface morphology. Results demonstrated that Panchina stone showed a high durability to the aging tests, and artificial degradation effects were not largely visible. The nanostructured products seem to be suitable for stone protection by virtue of their good compatibility and effectiveness.

Keywords: decay; stone protection; nanostructured products; aging test

Citation: Fernandez, F.; Germinario, S.; Montagno, R.; Basile, R.; Borgioli, L.; Laviano, R. Experimental Procedures of Accelerated Aging and Evaluation of Effectiveness of Nanostructured Products for the Protection of Volterra (Italy) Panchina Stone. *Buildings* **2022**, *12*, 1685. https://doi.org/10.3390/buildings12101685

Academic Editor: Cinzia Buratti

Received: 25 July 2022
Accepted: 9 September 2022
Published: 13 October 2022

1. Introduction

The aims of this work were to evaluate the effectiveness of nanostructured coatings for the protection of stone, in order to increase the stone durability, and to define experimental conditions and procedures of accelerated aging tests able to simulate different degradation environmental effects on the studied lithotype. The material identified for the experimentation was Panchina stone, coming from the historic walls of Volterra. The city of Volterra stands on the top of a hill located on the watershed between the valleys of the Era and Cecina rivers in Tuscany (Italy). Volterra was an important Etruscan city and, contrary to what happened to other cities in that historical period, it was also inhabited in the Roman and Middle Ages. Some ancient building works, such as the surrounding walls, were maintained because they were also used in the following centuries. The walls of the ancient city of Volterra were built for defensive purposes, probably in the 4th century BC and were restored from the Middle Ages to the present day; in fact, it is possible to recognize all the construction techniques occurring over time, but large tracts of the original walls still remain, in which it is possible to reconstruct the construction technique of the wall, formed mostly by large rough square stone blocks. Panchina stone is a yellowish

calcarenite stone, extracted in the Etruscan and Roman periods from quarries in western Tuscany, and widely used there as a building material, mainly in walls [1–6].

A typical outcrop of Panchina stone is located within the city of Livorno and belongs to the morpho-sedimentary element; it started developing around 125,000 years ago and is known in the literature as "Terrazzo di Livorno", as it represents the substrate on which the city was built [7–10].

It is a highly porous stone, with medium-sized grains, rich in organogenic carbonate fragments, mainly consisting in shells belonging to bivalves, gastropods, and echinoderms, visible to the naked eye or by using a lens [11].

Despite its good mechanical performance, this stone material is characterized by a considerable heterogeneity, with the presence of areas with high surface decohesion due to the action of rainwater, and the freezing and thawing process to which the stone is subject in the winter season in the area of Volterra [4–6]. In order to reduce differential degradation, it is advisable to treat the stone surfaces with a protective product that acts as a protective layer between the stone and the external agents. In the specific case of water, the protective coating can limit its interaction with the stone material, reducing the amount of water inside the porous structure of the material [12].

For this purpose, the research activity comprised experimentation on two innovative treatments for stone surfaces, capable of conferring a protective water-repellent effect on the surfaces, and the analysis of their behavior against accelerated aging, simulated in the laboratory, in order to increase their durability.

In the field of cultural heritage, polymeric films are commonly used to induce a water-repellent effect on the stone surface [13]. Acrylic polymers, siloxanes, fluoropolyethers and fluorinated acrylic polymers are usually used as hydrophobic coatings [14–16]. A main drawback of acrylic polymers (i.e., Paraloid B72) is their poor resistance to aging, especially to thermal and photooxidation processes [17,18]. On the other hand, siloxanes used as a protective coating on historic surfaces, demonstrated good chemical stability, due to their high strength Si-O bond, low surface tension and good resistance to thermal stress [19].

Fluoropolymers are chemically similar to polytetrafluoroethene (PTFE, or Teflon), which has hydrophobic and oleophobic properties. The early fluoropolymer coatings showed good results, but a low ability to bind to the stone; for this reason, special fluoropolymers containing functional groups (such as phosphates) were developed; these can adhere to the stone surface, consequently providing a more persistent protection [20,21]. However, these compounds are scarcely used, mainly because of their high cost. Recently, more resistant and economical fluorinated acrylics were synthetized [22].

In the last decade, some interesting solutions emerged from the field of nanotechnology and the application of nanoparticles [23]. Nanosized calcium hydroxide and silica were used for stone consolidation purposes, because of their high reactivity. Moreover, due to their reduced dimensions, these nanoparticles are able to penetrate deep into the stone structure [24–26]. Nanoparticles are also currently largely used and tested to improve the performance of protective coatings on stone surfaces, in order to enhance their performance in terms of resistance against water, biological attack and pollution [27]. Based on the features provided by the nanoparticles, these coatings can be grouped into superhydrophobic coatings and photocatalytic coatings [23].

In the first case, a self-cleaning effect occurs, in that dirt and early colonies of microorganisms do not adhere to the surface itself, but are generally "washed off" by the water. On a photoactive surface, in contrast, the organic matter adheres to the surface, but is easily oxidized and decomposed by the combination of light and photocatalysts [28].

In the scientific literature, coatings based on nanoparticles were successfully formulated and tested on several lithotypes, and a general improvement of the protection of the stone was stated [29–31].

Despite these results, the use of nanostructured coatings in the field of conservation of cultural heritage is still quite limited [32,33]. This is because data from long-term experimentation on the behavior of such materials are not yet available. These data are

fundamental if stakeholders are to understand the suitability of nanostructured coatings for the protection of built heritage, which should be preserved for as long as possible [23].

In this context, the aim of the research activities was to actively contribute to existing knowledge through the comparative evaluation of the effectiveness of two nanostructured coatings, testing their durability in the lab, in order to select the most suitable products. In addition, the research enabled the definition of the experimental conditions and procedures of an accelerated aging test, used to simulate different degradation environmental effects on the studied lithotype.

2. Materials and Methods

2.1. Stone Characterization

The characterization of the stone sample was performed on the material provided directly by Soprintendenza Archeologia, Belle Arti e Paesaggio di Pisa, collected directly on site from material resulting from the collapse of a portion of the walls located between Piazza Martiri della Libertà and Via dei Ponti in Volterra. The first phase mainly concerned the petrographic mineralogical characterization, X-ray diffractometry (XRD) and physical–mechanical parameters of the stone material, such as porosity, coefficient of water absorption by capillarity (Normal UNI EN 1925:2000) [34], permeability to water vapor (Normal 21/85 UNI EN 1015-19), [35,36] and the identification of the possible presence of soluble salts (Normal UNI 11087) [37] or alteration phenomena. The samples were cut into cubes measuring 5 × 5 × 5 cm, as indicated by the rules relating to the execution of the analyses. Water absorption tests were carried out after immersing the samples in water, according to the specifications of the UNI EN 12087 [38], before and after artificial aging. Furthermore, the water vapor permeability of the stone cubes was measured according to UNI EN 15803 [39]. In order to evaluate the durability of the stone, selected samples were subjected to different cycles of artificial aging to evaluate possible modifications upon exposure to thermo-hygrometric stress conditions, freezing/thawing, thermal shock and a salt spray chamber.

This aging methodology made it possible to evaluate the behavior of the treated materials to physical–mechanical stress determined by differential thermal expansion due to sudden changes in temperature, and to the physical–mechanical actions caused by the expansion of ice and salts inside the porous structure of the material [40,41]. The freeze/thaw test was conducted on all the treated and untreated samples and consisted in cyclically subjecting the samples to a phase of freezing in the freezer at a temperature of −20 °C and to a phase of thawing at 70 °C, passing through an intermediate temperature of +22 °C. Samples were subjected to a total of 7 cycles of aging. The thermal shock test, conducted on all the treated and untreated samples, consisted in cyclically subjecting them to a phase of freezing at a temperature of −20 °C and to a thawing phase at +22 °C, passing through an intermediate temperature +4 °C. Samples were subjected to 7 cycles of aging (Table 1):

Table 1. Accelerated aging program freeze/thaw and thermal shock.

FREEZE/THAW	THERMAL SHOCK
+22 °C, 1 h	−20 °C, 2 h
−20 °C, 3 h	+22 °C, 2 h
+22 °C, 1 h	+4 °C, 2 h
+70 °C, 3 h	

The third and last aging test consisted in the use of a saline spray chamber; the test was conducted on all the treated and untreated samples, following the normal standard (UNI EN 12370:2001) [42]. The salt spray test is an efficient method of the corrosion testing of various products, such as paints and coatings; it ensures the quality of the products and their ability to maintain the required performance under such working conditions for a

long time without being subjected to any damage or deformation. The test was performed for 21 days for a total of 21 aging cycles, with a concentration of 5% salt solution. Wetting characteristics were defined using a TQC Pocket Goniometer. The Pocket Goniometer PGX+ defines several surface properties for quality control. The instrument measures the dynamic and static contact angle of a standard liquid. PGX+ Pocket Goniometer conforms to all major international standards, including ASTM D724, and ASTM D5946 [43,44].

SEM-EDS electron microscopy was performed to investigate the possible penetration of salt particles within the porous structure of the stone material treated with the products, and their subsequent growth and development over time. All SEM-EDS electron microscopy analyses were carried out on the surface of the samples, in order to evaluate the behavior of the different treatments in relation to the surface morphology, and in section, with the aim of verifying the penetration of the treatments, respectively. To perform the sectional analysis, all the samples were incorporated in resin to prevent potential detachment of the treatments during the cutting and preparation of the samples; perfectly flat surfaces were obtained, which limited potential optical distortions during observations under the microscopy [45].

2.2. Applied Products

Two innovative products, covered by an industrial patent, were applied and tested: NSW, a concentrated aqueous dispersion of functionalized silica nanoparticles and NSO, an aqueous dispersion of nanometric fluorosilanes.

As regards the NSW, silica nanoparticles are good candidates for such applications due to their low cost of fabrication, their ready availability and the ability to modify their surfaces by known chemical methods. The surface modification of silica nanoparticles allows control over their hydrophilicity and also improvement of their salt tolerance.

Silica nanoparticles are silicon dioxide (SiO_2) particles, spherical in shape and with a diameter between 5 and 100 nm. Depending on the way they are produced, silica nanoparticles, always in the form of aqueous dispersions, can be:

- Monodisperse (with a very narrow particle-size distribution);
- Polydisperse (with a wider dimensional distribution).

Once penetrated into the porous structure of a material, and the water evaporated, the silica nanoparticles react both with the hydroxyl groups present on the stone surfaces, and with each other, forming silica polymers, similarly to what happens with the best known and most widely used consolidant, ethyl silicate [46]. There are dozens of types of silica nanoparticle dispersion, different in the size and distribution of particles, stabilization methods and the presence of additives of various types, but only a few yielded appreciable results for the restoration sector [13,31,47].

As regards the nanometric fluorosilanes NSO, the replacement of hydrogen (H) atoms with fluorine (F) atoms in a polymeric structure enhances its ability to endure heat, light, flame, moisture or chemicals [48,49].

Moreover, F atoms reduce the surface energy of the material, hence, increasing hydrophobicity. For these reasons, fluorinated polymers were extensively investigated and suggested for use in the conservation of buildings and objects of cultural heritage exposed to atmospheric conditions [50,51].

Both products were applied by brush (Figure 1): in particular, NSW was diluted with distilled water in a ratio of 1:1, while NSO was applied as it was.

2.3. Comparative Testing of Treatments

The comparative testing of treatments performed on the surface of the samples was divided into three phases. The first phase involved an accurate macroscopic and microscopic analysis of all the surfaces of the treated and untreated samples. Surface wettability measurements were carried out by measuring the contact angle, evaluating the constant mass of the samples with an analytical balance and determining the absorption of H_2O by capillarity (NORMAL 11/85) [52].

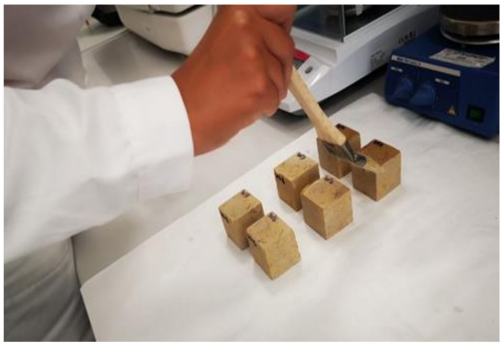

Figure 1. Application phase.

During the second phase, different accelerated aging tests were conducted to highlight, in advance, not only the behavior of the samples to hygrothermal shocks, but also any possible surface alterations due to the applied treatments. Before and after the different aging tests, the measurement of the contact angle with the Pocket Goniometer TQC (TAPPI T458, ASTM D724, ASTM D5946) [43,44] and the water absorption by capillarity (UNI EN 1925:2000), [34], were performed on each sample; the water repellency conferred to the surfaces by the two coatings and the improvement over the untreated samples were then comparatively evaluated. In the third phase, all the measurements from the first phase were repeated and scanning electron microscopy (SEM-EDS) analyses were carried out to evaluate the behavior of the different treatments in relation to the surface morphology of the samples, and in section, to verify the penetration of treatments.

3. Results and Discussion

3.1. Stone Characterization

Observation of the thin sections revealed that the rock in question is a clastic sedimentary rock consisting of carbonate and silicate granules. The carbonate component is represented by bioclasts (fragments of molluscs, echinoderms, calcareous algae, bryozoans, macroforaminifera) and by lithoclasts with a microsparitic to micritic texture. The silicate component is represented by granules of quartz, feldspar (plagioclase, orthoclase and microcline), gneissic lithics and subordinate granules of mica, chlorite and iron oxides. The latter appear as segregations in the chloritic granules or as late diagenesis fillings in the inter and intragranular voids.

The particle size of the clasts, both silicate and carbonate, is mainly between 0.2 and 0.4 mm, with a maximum size of 0.8 mm. Sporadically, centimeter-sized lamellibranch shells are observed.

The optical microscope observation showed the high compactness of the matrix and the presence of silicate clasts (quartz, feldspar, mica) and carbonate clasts (bioclasts) cemented by spathic calcite. In the intergranular voids not occluded by the calcitic cement, secondary filling of iron oxides was also noted (Figures 2 and 3).

In summary, it can be said that, from the petrographic point of view, the material can be considered an arcosic litoarenite, a clastic sedimentary rock with calcitic cement.

Diffractometry, as shown in the Figure 4 below, revealed 30% quartz, 60% calcite, 9% feldspar and 1% mica.

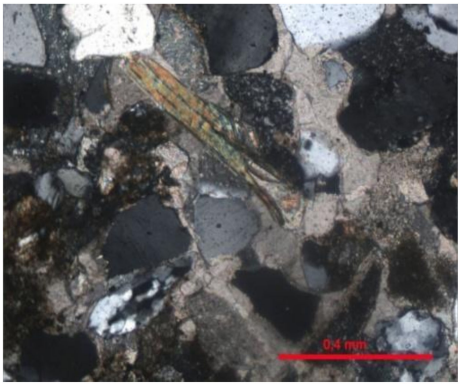

Figure 2. Thin section observations.

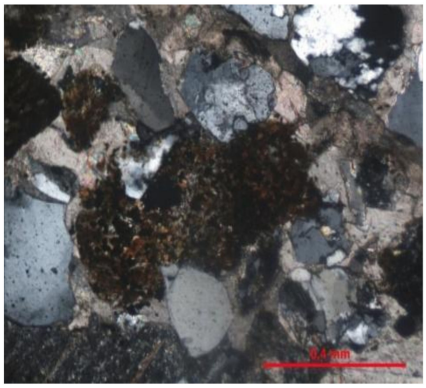

Figure 3. Thin section observations.

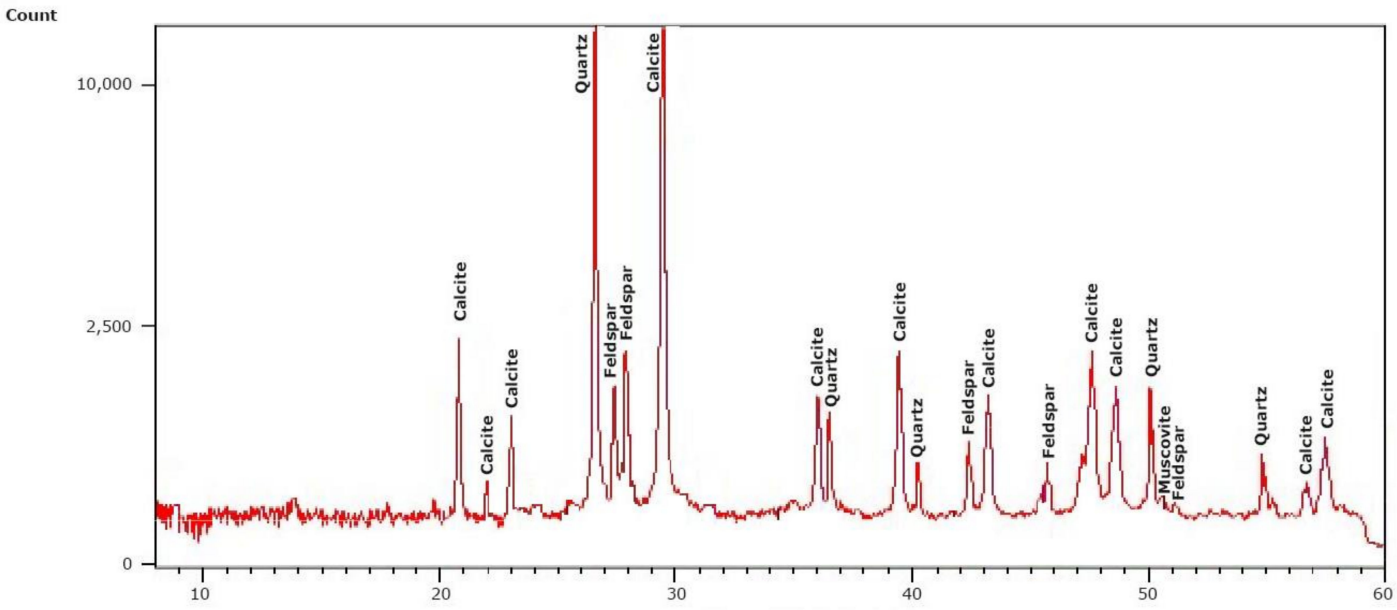

Figure 4. Diffractometry on the stones.

From the interpretation of the other analyses performed on the stone material (uniaxial mechanical resistance, UNI EN 1926: 2007 standard [53]; water absorption by capillarity UNI EN 1925: 2000 standard; permeability to water vapor, UNI EN ISO 7783 standard) [54], it is clear that it is a rock characterized by high compactness, deductible from the low average value of total porosity (5.9%), high mechanical resistance to uniaxial compression (72 MPa 72 N/mm^2), low water absorption coefficient by capillarity (CW, S between 11.56

and 4.83 g/(m^2 × s$^{0.5}$)) and low vapor permeability (μ 116.4). There is also an absence of soluble salts, such as sulphates, and the irrelevant presence of chlorides (0.21%). The rock, however, did show sporadic areas of lower cementation and, therefore, reduced compactness and greater porosity.

3.2. Comparative Testing of Treatments

The water absorption test by capillarity, conducted on the samples (5 × 5 × 5 cm), treated just on one face (1F) or six faces (6F), shows that in the first ten minutes of treatment the quantity of water absorbed was greater than 25% of the total quantity of water absorbed after 8 days of absorption, showing a slow but progressive imbibition capacity (Figure 5).

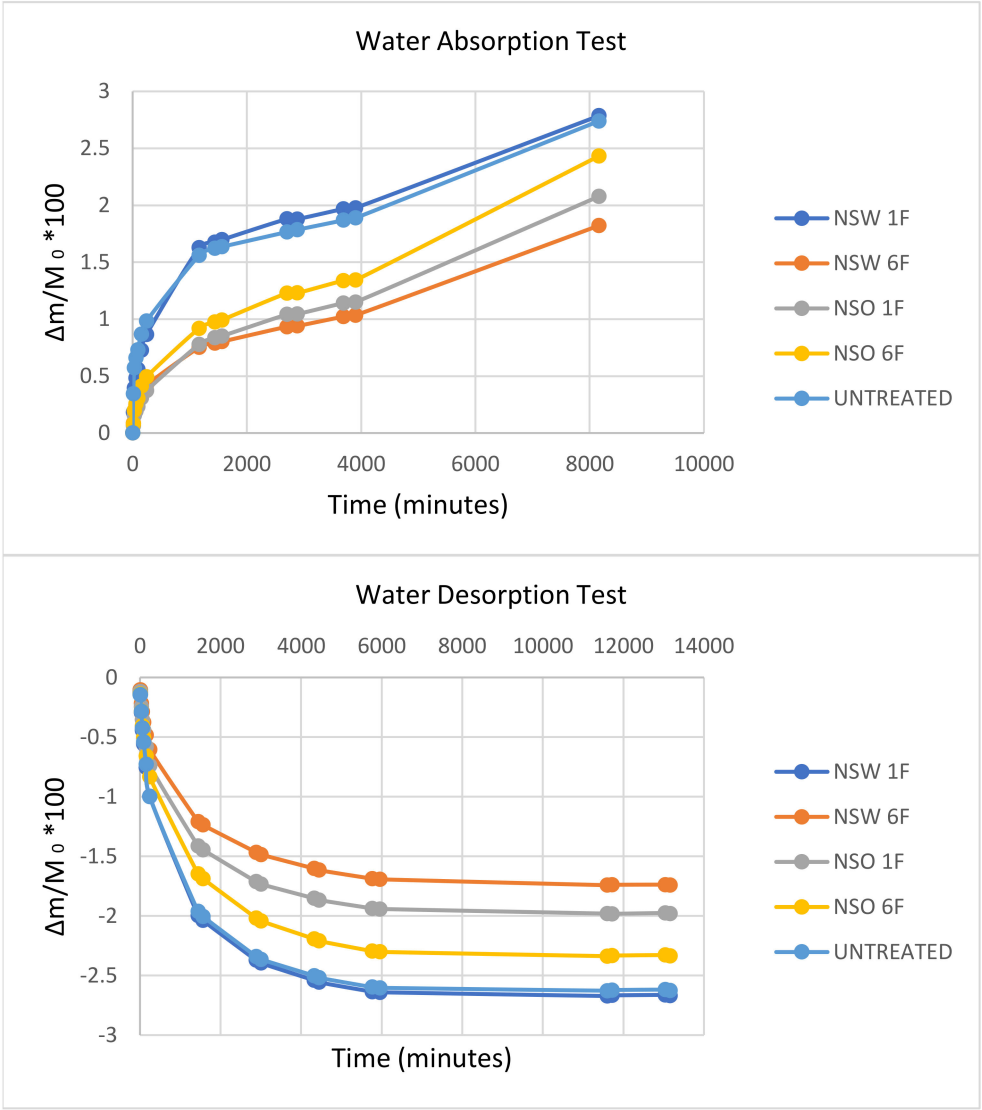

Figure 5. Water Absorption and Desorption Tests.

At the end of each absorption cycle, and for each of the three aging processes used, the following change in index parameters selected were evaluated: the measurement of the *contact angle*, *shape differences*, *surface degradation* and *rate mass loss of the samples*.

The results of the three accelerated aging tests show that, macroscopically, the samples maintained an intact shape and external aspect, and showed no evident marker of deterioration; furthermore, the mass loss was insignificant, at less than 1%.

3.3. Contact Angle Measurement

The results, relating to a 4 µL drop, at 24 h, 48 h and 30 days from application, are shown in the following table (Table 2).

Table 2. Contact angle measurement.

Sample Name	Applied Product (2 Coats)	Note	Contact Angle 24 h	Contact Angle 48 h	Contact Angle 30 Days
V01	NSO	1F	81.10	90.60	85.57
V02	NSO	1F	90.13	87.70	89.50
V03	-	REF. SAMPLE	-	-	-
V04	NSO	1F	84.40	73.80	85.60
V05	NSO	1F	89.70	90.33	88.60
V06	NSO	1F	81.87	85.73	85.80
V07	NSO	1F	81.33	85.60	86.70
V08	NSO	6F	78.60	91.12	90.57
V09	NSO	6F	85.78	88.28	89.38
V010	-	REF. SAMPLE	-	-	-
V011	NSO	6F	86.60	85.32	88.08
V012	NSW	1F	76.93	69.70	83.07
V013	NSW	1F	78.77	83.10	80.70
V014	NSW	1F	84.83	85.87	79.30
V015	NSW	1F	63.93	85.43	84.60
V016	-	REF. SAMPLE	-	-	-
V017	-	REF.	-	-	-
V018	NSW	1F	74.90	90.30	81.17
V019	-	REF. SAMPLE	-	-	-
V020	NSW	1F	86.00	73.50	77.70
V021	NSW	6F	75.85	79.97	83.67
V022	NSW	6F	88.65	84.85	86.65
V023	NSW	6F	70.47	78.64	78.98
1	NSO	1F	86.77	86.17	85.83
2	NSO	1F	83.13	76.97	87.50
3	NSW	1F	82.53	88.63	90.87
4	NSW	1F	83.50	83.47	84.33
5	-	REF. SAMPLE	-	-	-
6	-	REF. SAMPLE	-	-	-

Figure 6 shows the difference of the behavior of the surface, before and after the treatment and the aging tests.

The average values of the wettability measurements of the analyzed samples, differentiated by coating, are listed below, in the Table 3:

Table 3. Average values of the wettability measurements.

Sample Name	Applied Product (2 Coats)	Average Value 24 h	Average Value 48 h	Average Value 30 Days
V01	NSO	84.76	85.63	86.96
V02	NSO			
V04	NSO			
V05	NSO			
V06	NSO			
V07	NSO			
V08	NSO	83.66	88.24	89.34
V09	NSO			
V011	NSO			

Table 3. *Cont.*

Sample Name	Applied Product (2 Coats)	Average Value 24 h	Average Value 48 h	Average Value 30 Days
V012	NSW	77.56	81.32	81.09
V013	NSW			
V014	NSW			
V015	NSW			
V018	NSW			
V020	NSW			
V021	NSW	78.32	81.15	83.10
V022	NSW			
V023	NSW			

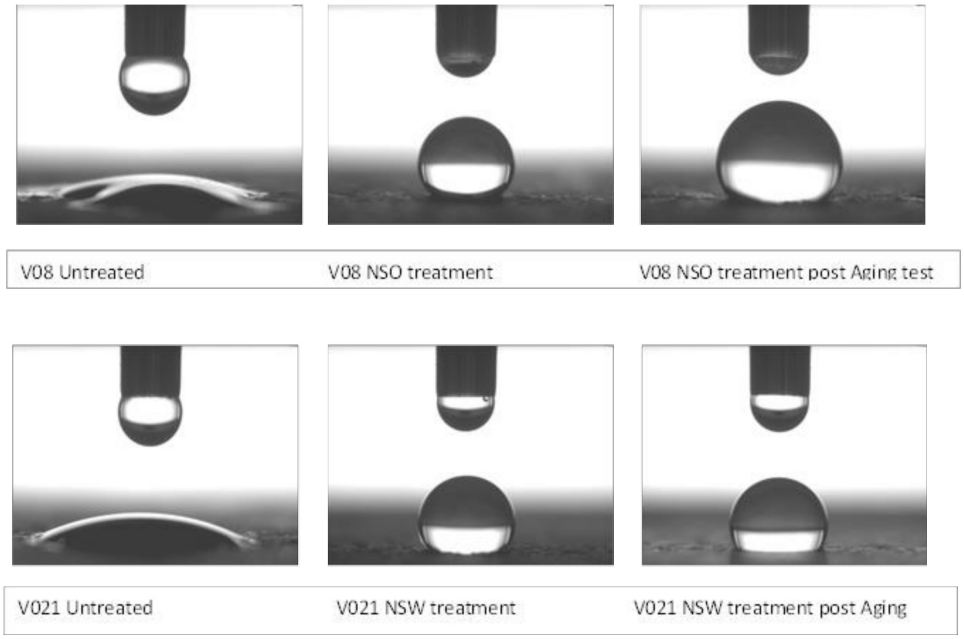

Figure 6. Contact angle measurement.

The same measurements were performed after the water desorption test and, in both cases, the contact angles observed on NSO surfaces were higher than on NSW surfaces.

3.4. Durability Characteristics

Compared with other protocols available in the literature [55,56], that proposed here is marked by a systematic investigation into the effects of thermo-hygrometric stress, by freezing/thawing, thermal shocks and a salt spray chamber. This aging methodology made it possible to specifically evaluate the behavior of the treated materials to physical-mechanical stress determined by differential thermal expansion due to sudden changes in temperature and to the physical-mechanical actions caused by the expansion of ice and salts inside the stone porous structure.

In particular, the results obtained after aging with the freeze/thaw test and thermal shock test show that the samples macroscopically preserved their shape and external aspect, without showing evident signs of deterioration. These results could be referred to as high mechanical resistance of the stone and good distribution of the products, which did not affect the behavior of the stone. Moreover, the contact angles measured at the end of the accelerated aging tests showed a slight decrease compared with those taken initially.

The samples subjected to the salt spray chamber showed lower contact angle measurements after this test, with an average value of 75° for both products. It is reasonable to

assume that the presence of aggressive environments containing a marine aerosol resulted in a slight decrease in the hydrophobic performances of the treated surfaces. Even with this slight reduction, comparing the untreated sample, the protective effect is still active, since contact angles of approximately 80° were obtained on the treated surfaces.

We deduce that, as in the case of Roverio et al. [57], when the products are able to penetrate deeply enough inside the stone pores, they retain much of their hydrophobic properties, even after partial chemical degradation of the matrices has occurred on the actual stone surface.

3.5. SEM-EDS Analysis

The results of SEM-EDS analyses show a good compatibility between the surfaces of the samples and the treatments applied. In particular, in the sample where the NSO (based on fluorosilanes) treatment was applied, the elemental analysis confirms the presence of the treatment on the surface after the aging cycles: in fact, the intensity of the fluorine appears very marked. The observations relative to the surface morphology after application and the aging of the samples show that the applied product followed the surface morphology perfectly (Figures 7 and 8).

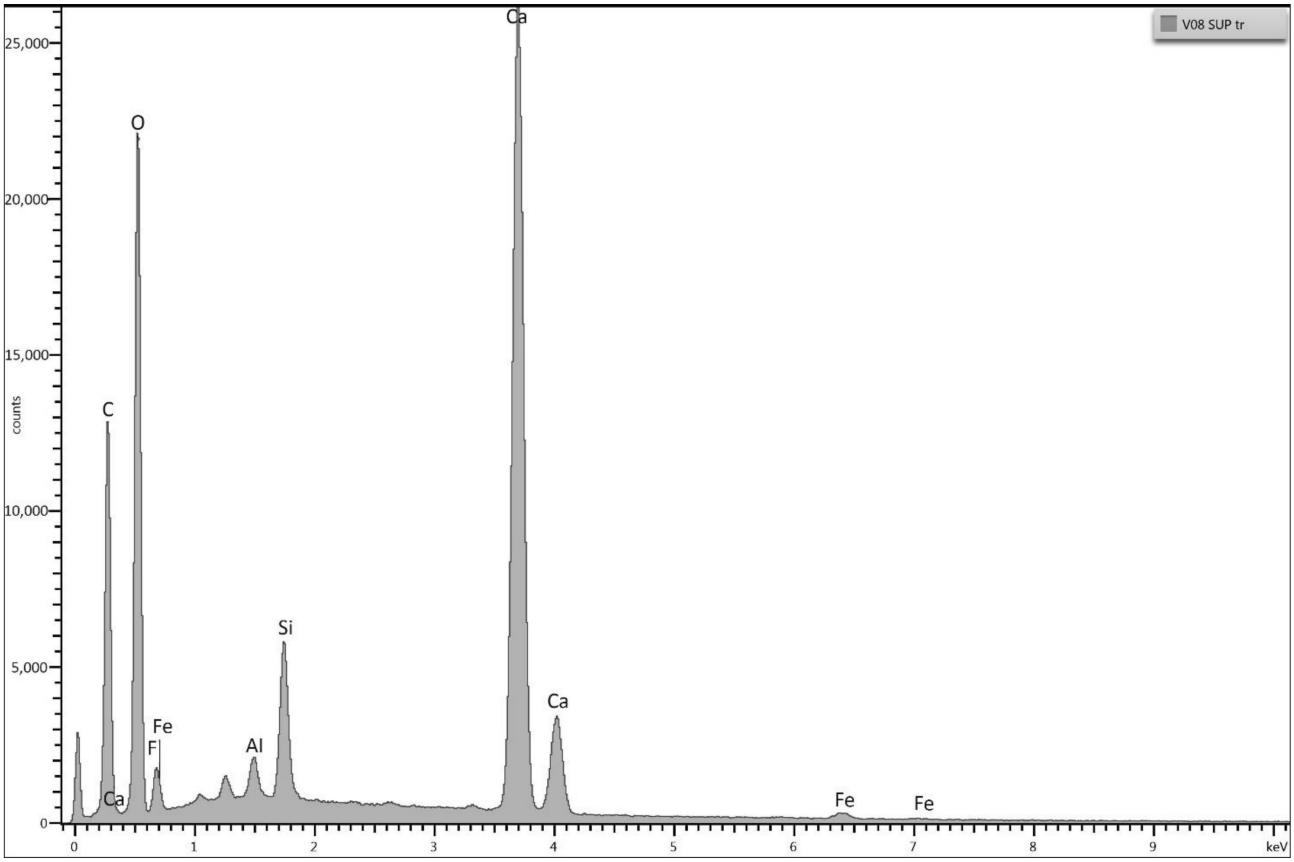

Figure 7. Elemental analysis in SEM-EDS: sample treated with NSO (University of Bari Aldo Moro).

The analysis of the sample in the section mapping shows the penetration of fluorine after aging and the point elemental analysis confirms the presence of the treatment (Figure 9).

The results of the SEM-EDS analysis on the sample surface where the NSW treatment based on functionalized silica nanoparticles was applied show the presence of the treatment in the sample. The elemental analysis conducted on the surface of the sample confirms, however, a marked presence of silicon, despite the substrate of the sample still having a very high quartz component (Figure 10).

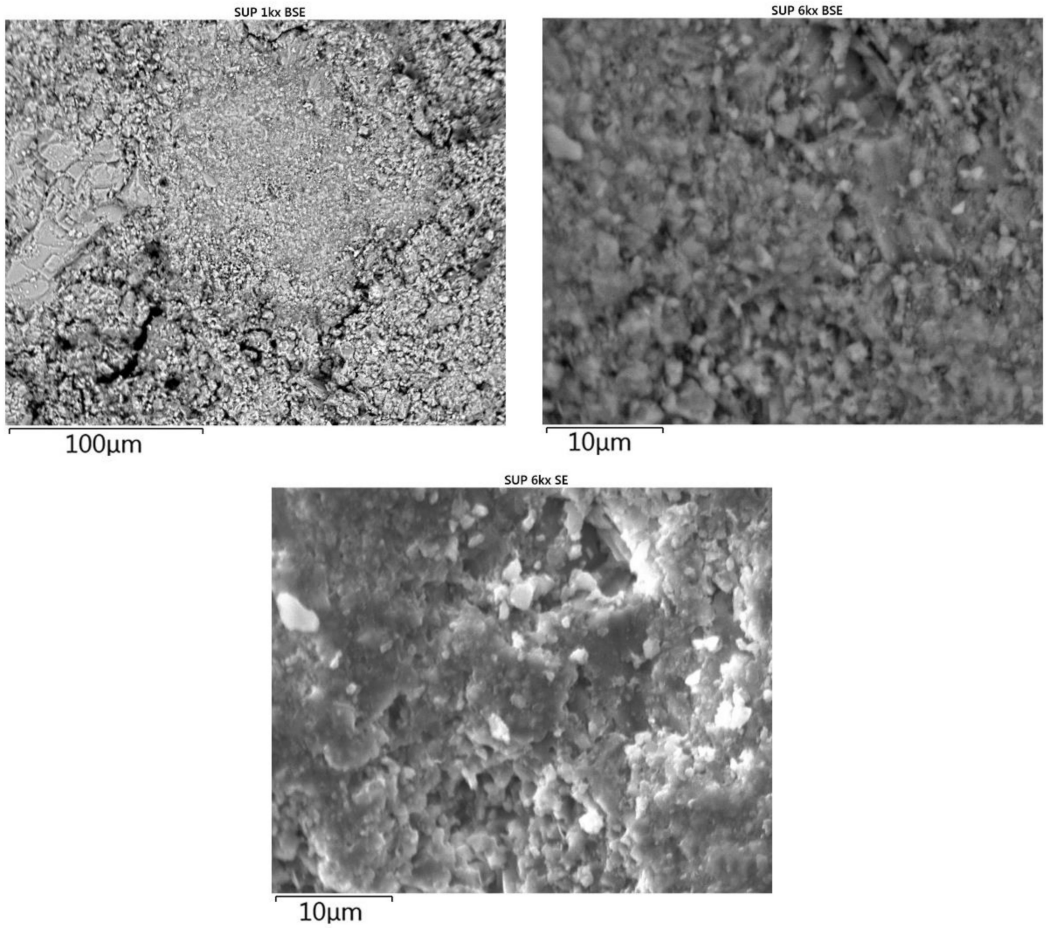

Figure 8. SEM-EDS images: Morphology of the sample surface after application of the NSO product (University of Bari Aldo Moro).

The images of the surface morphology also show the absence of product thickening, which is evidence that the product has penetrated without changing the surface texture of the substrate (Figure 11).

In addition, the analysis relating to section mapping confirms the marked presence of silicon within the sample, while the point elemental analysis confirms the presence of the silicon marker of the treatment, and also a component of the substrate (Figure 12).

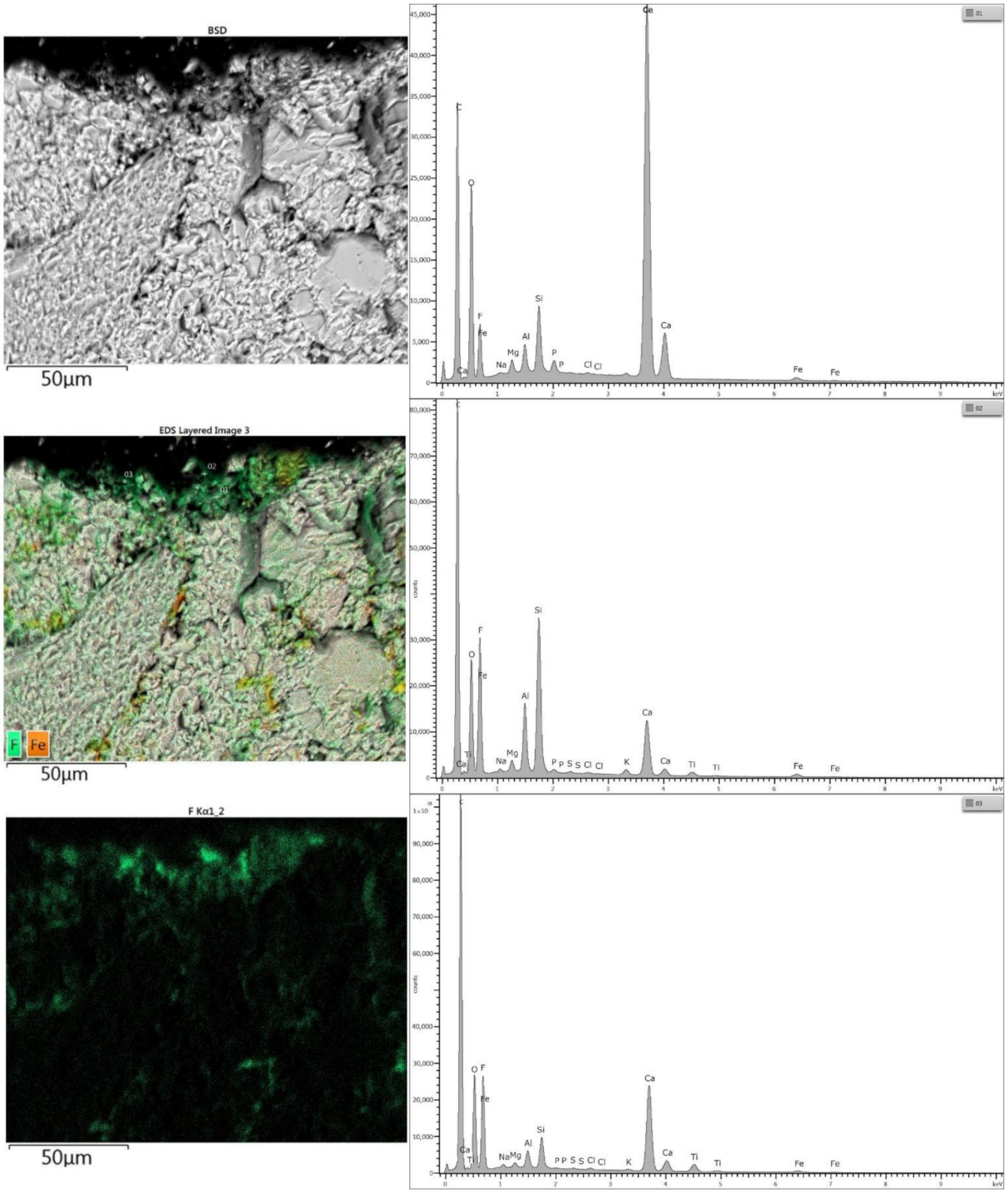

Figure 9. SEM-EDS images: Section mapping and point elemental analysis: sample treated with NSO product (University of Bari Aldo Moro).

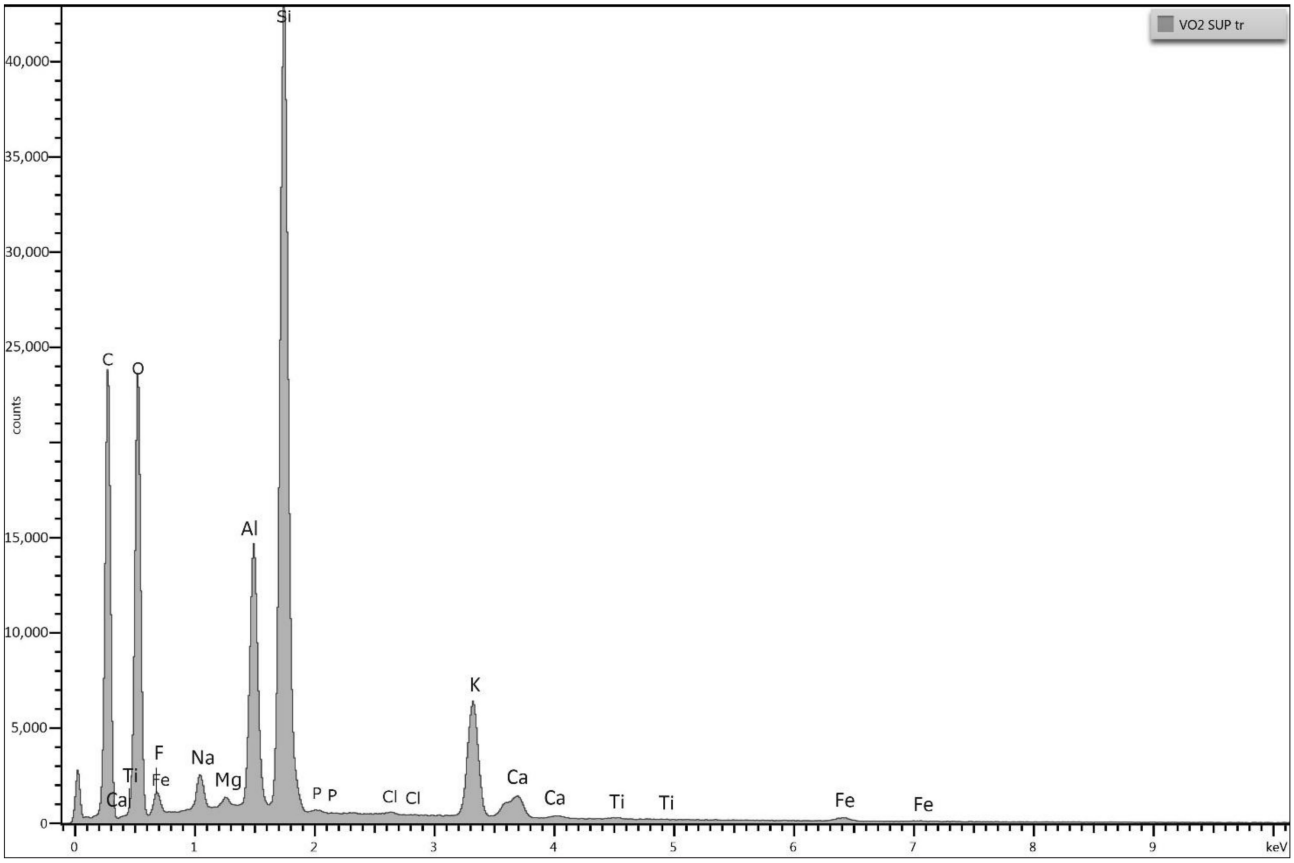

Figure 10. Elemental analysis in SEM-EDS: sample treated with NSW treatment (University of Bari Aldo Moro).

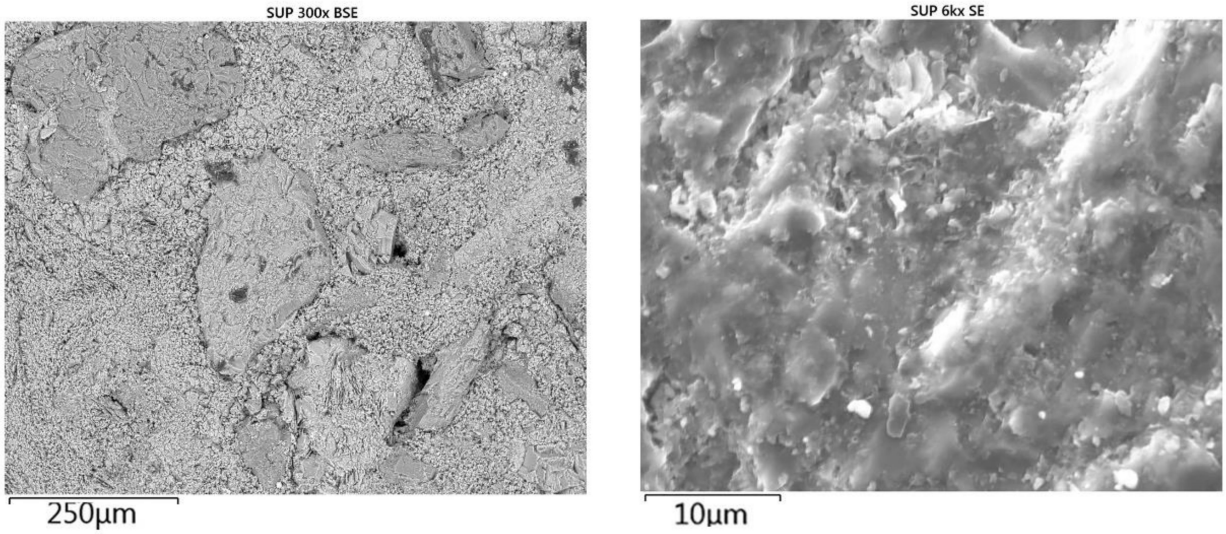

Figure 11. SEM-EDS images: Morphology of the sample surface after application of product NSW (University of Bari Aldo Moro).

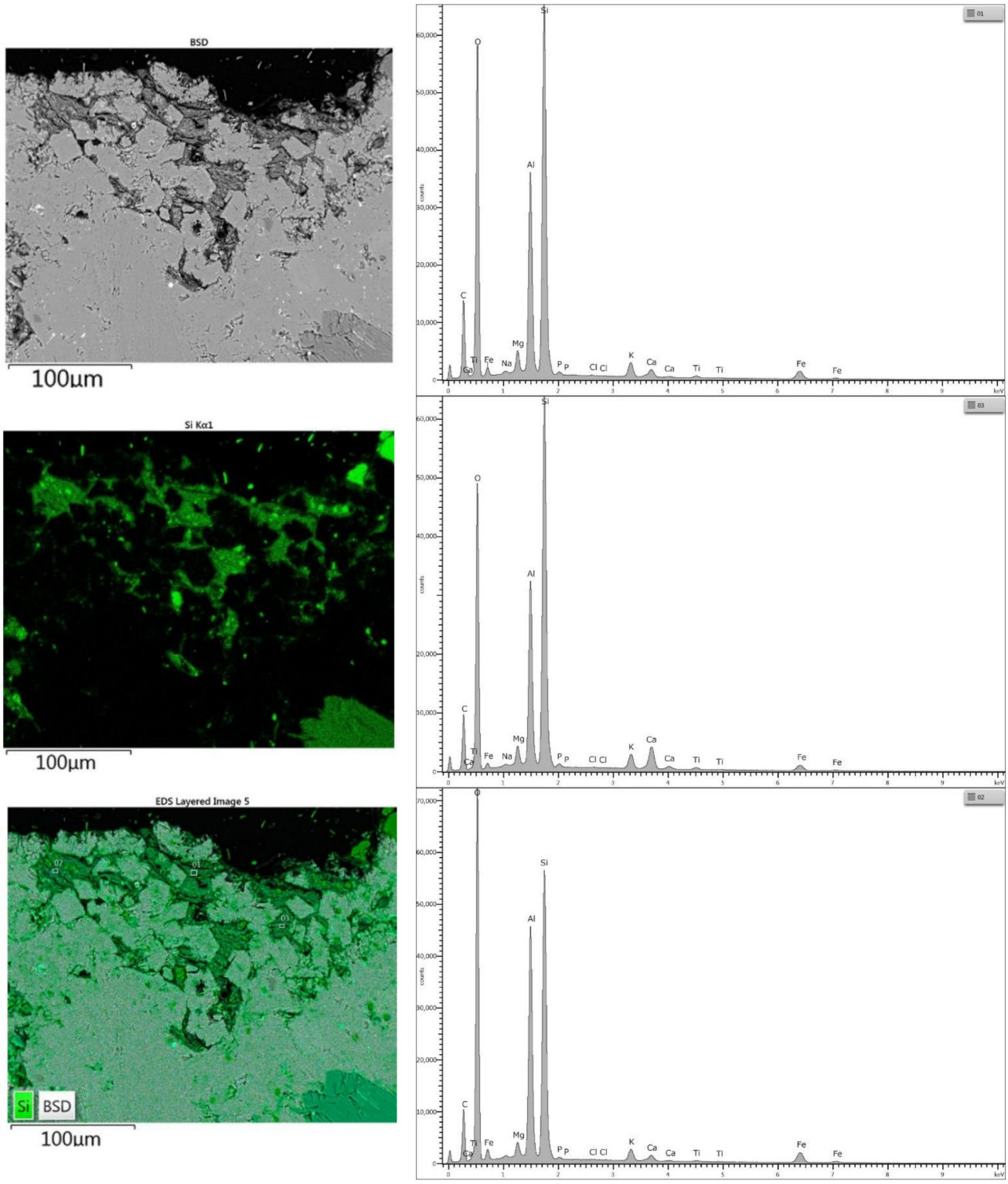

Figure 12. SEM-EDS images: Section mapping and point elemental analysis, sample treated with product NSW (University of Bari Aldo Moro).

4. Conclusions

The activities and tests conducted enabled the testing of stone samples treated with two different products for the protection of the stone material. In particular, from the microscopic observations of the treated surfaces, no alterations were detected after the

application of the products, nor after the water absorption and desorption processes, despite the prolonged contact with water of the surfaces of the samples.

With regard to the surface wettability measurements, after application and before aging, the measurements made at 24–48 h and after 30 days demonstrate that the samples with the highest contact angle and, therefore, the most hydrophobic surface, are those treated with NSO, even though NSW still shows good values.

Following the aging of the samples with freeze-thaw cycles, the results relating to the loss in mass show that the treated samples exhibit good resistance: no abnormal behavior, surface loss of cohesion, fractures or mass loss were detected. As regards the post freeze-thaw wettability measures, there is also good maintenance of performance in terms of surface-water repellency. Following aging of the samples with thermal shock cycles, the results relating to the loss in mass show that the treated samples have good resistance over time: there is no weight reduction, and no anomalous behavior, surface loss of cohesion or fractures were detected. As regards the post thermal shock wettability measures, again, there is good maintenance of performance in terms of surface-water repellency. Even after aging with salt spray cycles, on average, none of the samples loses mass. As regards the post-salt spray wettability measures, on the other hand, there is a slight deterioration, despite the surfaces continuing to maintain good water repellency. It is, therefore, noted that, among phenomena simulated in the laboratory, the most "aggressive" for the treated stone is most likely the action of the salts.

The SEM-EDS investigations made it possible to verify a good homogeneity of distribution of the products within the porous structure of the material, as well as the absence of by-products or alterations that could have been caused by the natural aging to which the samples had been subjected. The SEM observations revealed that the two products did not create any film and they did not alter the substrate. It is also noted that, despite having been subjected to prolonged action of saline mist, in the elemental mapping in section, the presence of NaCl was not detected at depth. This suggests that both protective agents performed their function, preventing the saline solution from penetrating the surface; the salts, therefore, remained on the surface and were then easily washed away.

The developed aging protocol produced positive and significant results; it could, therefore, be replicated for the evaluation of other products on stone materials with characteristics similar to those of Panchina stone.

Furthermore, in order to complete this study and expand the multiparametrical evaluation essential for the most effective conservation of the material, the evaluation will continue with analysis of the combined UV and humidity effects. Variations in the parameters under investigation in the climatic chamber will allow the evaluation of the incidence and combination of the two parameters on the behavior and durability of the treatments. Nevertheless, in the future, the durability and the behavior of the coatings after prolonged natural aging should be tested directly on pilot sites.

Author Contributions: All authors listed have made a substantial, direct and intellectual contribution to the work, and approved it for publication. Conceptualization, F.F., L.B. and R.L.; Methodology, F.F. and S.G.; Investigation, F.F., S.G., R.M. and R.B.; Data Curation S.G., R.M. and R.B.; Writing—Original Draft Preparation, F.F., S.G., R.M. and R.B.; Writing—Review and Editing, F.F., S.G. and R.M.; Supervision, F.F.; Project Administration, R.M. All authors have read and agreed to the published version of the manuscript.

Funding: This research was funded by I.E.ME.S.T., in the framework of the collaboration between the Research Institute, Università degli Studi di Palermo, Università degli Studi di Bari Aldo Moro and CTS, leader in the field of Restoration, Conservation and Storage of historical, artistic, monumental, works of arts.

Institutional Review Board Statement: Not applicable.

Informed Consent Statement: Not applicable.

Data Availability Statement: Data supporting reported results can be found in I.E.ME.S.T.

Conflicts of Interest: The authors declare no conflict of interest.

References

1. Cristofani, M. Volterra. Scavi 1969–1971. *Not. Scavi Antich.* **1973**, *28*, 13–245.
2. Cristofani, M. Volterra. Scavi nella necropoli del Portone. *NS* **1955**, *29*, 114–181.
3. Cristofani, M. *L'Acropoli di Volterra: Nascita e Sviluppo di Una Città*; Pacini Editore: Pisa, Italy, 1981.
4. Dennis, G. *Volterra: Città e Necropoli d'Etruria. A Cura di G. Cateni*; NIE Editore: Siena, Italy, 1986.
5. Fiumi, E. Contributo alla datazione del materiale volterrano: Gli scavi della necropoli del Portone negli anni 1873–1874. *Stud. Etruschi* **1957**, *25*, 367–415.
6. Bruun, P. Studies in de romanisation of Etruria. *Acta Inst. Rom. Finl. Bardi Ed. Roma* **1975**, *5*, 518.
7. Rodolico, F. *Le Pietre delle Città d'Italia*; Le Monnier: Firenze, Italy, 1953.
8. Malatesta, A. Le formazioni pleistocenice del Livornese. *Atti. Soc. Tosc. Sci. Nat. Mem. Ser. A* **1942**, *51*, 145–206.
9. Barsotti, G.; Federici, P.R.; Antonioli, F.; Silenzi, S.; Vittori, E.; Villani, C. Sea level changes and tectonic mobility. Precise measurements in three coastlines of Italy considered stable during the last 125 ky. *Phys. Chem. Earth Part A Solid Earth Geod.* **1999**, *24*, 337–342.
10. Giannelli, L.; Mazzanti, R.; Salvatorini, G. Studio del Quaternario Livornese, con particolare riferimento alla stratigrafia e alle faune delle formazioni del bacino di carenaggio della Torre del Fanale. *Mem. Soc. Geol. Ital.* **1974**, *13*, 425–495.
11. Aquino, A.; Pagnotta, S.; Polese, S.; Tamponi, M.; Lezzerini, M. Panchina Calcarenite: A Building Material from Tuscany Coast. *Earth Environ. Sci. 6th World Multidiscip. Earth Sci.* **2020**, *5*, 609. [CrossRef]
12. Price, C.A.; Doehne, E. *Stone Conservation: An Overview of Current Research*; Getty Conservation Institute: Los Angeles, LA, USA, 2011.
13. Manoudis, P.N.; Papadopoulou, S.; Karapanagiotis, I.; Tsakalof, A.; Zuburtikudis, I.; Panayiotou, C. Polymer-Silica nanoparticles composite films as protective coatings for stone-based monuments. *J. Phys. Conf. Ser.* **2007**, *61*, 1361–1365. [CrossRef]
14. Delgado-Rodriguez, J. Consolidation of decayed stone. A delicate problem with few practical solutions, Historical constructions. In Proceedings of the International Seminar on Historical Constructions, Guimarães, Portugal, 7–9 November 2001.
15. Rizzarelli, P.; La Rosa, C.; Torrisi, A. Testing a fluorinated compound as a protective material for calcarenite. *J. Cult. Herit.* **2001**, *2*, 55–62. [CrossRef]
16. Poli, T.; Toniolo, L.; Chiantore, O. The protection of different Italian marbles with two partially fluorinated acrylic copolymers. *Appl. Phys. A* **2004**, *79*, 347–351. [CrossRef]
17. Lazzari, M.; Chiantore, O. Thermal-ageing of paraloid acrylic protective polymers. *Polymer* **2000**, *41*, 6447–6455. [CrossRef]
18. Chiantore, O.; Lazzari, M. Photo-oxidative stability of paraloid acrylic protective polymers. *Polymer* **2001**, *42*, 17–27. [CrossRef]
19. Lazzarini, L.; Laurenzi Tabasso, M. *Il Restauro della Pietra*; CEDAM: Padova, Italy, 1994.
20. Aglietto, M.; Passaglia, E.; Taburoni, E.; Ciardelli, F.; Botteghi, C.; Matteoli, U. A new class of fluorinated acrylic polymers: Protective materials for stone. In Proceedings of the ICOM Commitee for Conservation: 10th Triennal Meeting, Washington, DC, USA, 20–27 August 1993; Volume 2, pp. 553–558.
21. Gu, J.-D. Microbiological deterioration and degradation of synthetic polymeric materials: Recent research advances. *Int. Biodeterior. Biodegrad.* **2003**, *52*, 69–91. [CrossRef]
22. Sabatini, V.; Farina, H.; Montarsolo, A.; Pargoletti, E.; Ortenzi, M.A.; Cappelletti, G. Fluorinated polyacrylic resins for the protection of cultural heritages: The effect of fluorine on hydrophobic properties and photochemical stability. *Chem. Lett.* **2018**, *47*, 280–283. [CrossRef]
23. Ruffolo, S.A.; La Russa, M.F. Nanostructured Coatings for Stone Protection: An Overview. *Front. Mater.* **2019**, *6*, 147. [CrossRef]
24. Baglioni, P.; Giorgi, R. Soft and hard nanomaterials for restoration and conservation of cultural heritage. *Soft Matter* **2006**, *2*, 293–303. [CrossRef]
25. Rodriguez-Navarro, C.; Ruiz-Agudo, E. Nanolimes: From synthesis to application. *Pure Appl. Chem.* **2017**, *90*, 523–550. [CrossRef]
26. Pozo-Antonio, J.S.; Otero, J.; Alonso, P.; Barberà, X. Nanolime- and nanosilica-based consolidants applied on heated granite and limestone: Effectiveness and durability. *Constr. Build. Mater.* **2019**, *201*, 852–870. [CrossRef]
27. Ruffolo, S.A.; La Russa, M.F.; Malagodi, M.; Oliviero Rossi, C.; Palermo, A.M.; Crisci, G.M. ZnO and $ZnTiO_3$ nanopowders for antimicrobial stone coating. *Appl. Phys. A Mater. Sci. Process.* **2010**, *100*, 829–834. [CrossRef]
28. La Russa, M.F.; Rovella, N.; De Buergo, M.A.; Belfiore, C.M.; Pezzino, A.; Crisci, G.M. Nano-TiO_2 coatings for cultural heritage protection: The role of the binder on hydrophobic and self-cleaning efficacy. *Prog. Org. Coat.* **2016**, *91*, 1–8. [CrossRef]
29. Bergamonti, L.; Predieri, G.; Paz, Y.; Fornasini, L.; Lottici, P.P.; Bondioli, F. Enhanced self-cleaning properties of N-doped TiO_2 coating for Cultural Heritage. *Microchem. J.* **2017**, *133*, 1–12. [CrossRef]
30. Banerjee, S.; Dionysiou, D.D.; Pillai, S.C. Self-cleaning applications of TiO_2 by photo-induced hydrophilicity and photocatalysis. *Appl. Catal. B Environ.* **2015**, *176–177*, 396–428. [CrossRef]
31. De Ferri, L.; Lottici, P.P.; Lorenzi, A.; Montenero, A.; Salvioli-Mariani, E. Study of silica nanoparticles—Poly-siloxane hydrophobic treatments for stone-based monument protection. *J. Cult. Herit.* **2011**, *12*, 356–363. [CrossRef]
32. Simpson, J.T.; Hunter, S.R.; Aytug, T. Superhydrophobic materials and coatings: A review. *Rep. Prog. Phys.* **2015**, *78*, 8. [CrossRef]
33. Crupi, V.; Fazio, B.; Gessini, A.; Kis, Z.; La Russa, M.F.; Majolino, D. TiO_2-SiO_2-PDMS nanocomposite coa-ting with self-cleaning effect for stone material: Finding the optimal amount of TiO_2. *Constr. Build. Mater.* **2018**, *166*, 464–471. [CrossRef]

34. *UNI EN 1925*; Metodi di Prova Per Pietre Naturali—Determinazione del Coefficiente di Assorbimento d'Acqua per Capillarità. Ente Nazionale Italiano di Unificazione: Milano, Italy, 2000.
35. *Normal 21/85*; Permeabilità Al Vapor d'Acqua. CNR-ICR: Rome, Italy, 1987.
36. *UNI EN 1015-19*; Metodi di Prova per Malte per Opere Murarie—Determinazione della Permeabilità Al Vapore d'Acqua delle Malte da Intonaco Indurite. ISO: Geneva, Switzerland.
37. *UNI 11087*; Beni Culturali—Materiali Lapidei Naturali Ed Artificiali—Determinazione del Contenuto di Sali Solubili. ISO: Geneva, Switzerland.
38. *UNI EN 12087*; Isolanti Termici Per Edilizia—Determinazione dell'Assorbimento d'Acqua a Lungo Termine: Prova Attraverso Immersione. ISO: Geneva, Switzerland, 2013.
39. *UNI EN 15803*; Conservazione dei Beni Culturali—Metodi di Prova—Determinazione della Permeabilità Al Vapore d'Acqua (dp). ISO: Geneva, Switzerland, 2010.
40. Germinario, S. Analysis of leccese stone decay after laboratory ageing test. In Proceedings of the VIIth Conference Diagnosis, Conservation and Valorization of Cultural Heritage, Napoli, Italy, 15–16 December 2016; pp. 252–258.
41. Fernandez, F.; Germinario, S. Alteration and deterioration of natural stone materials: Artificial aging as a tool of knowledge. In Proceedings of the VIIIth Conference Diagnosis, Conservation and Valorization of Cultural Heritage, 14–15 December 2017; pp. 324–333.
42. *EN 12370*; Metodi di Prova per Pietre Naturali. Determinazione della Resistenza Alla Cristallizzazione dei Sali. CNR-ICR: Rome, Italy, 2001.
43. *ASTM D724-99*; Standard Test Method for Surface Wettability of Paper (Angle-of-Contact Method). ASTM: West Conshohocken, PA, USA, 2003.
44. *ASTM D5946*; Standard Test Method for Corona-Treated Polymer Films Using Water Contact Angle Measurements. ASTM: West Conshohocken, PA, USA, 2004.
45. Adams, A.E.; Mackenzie, W.S. *A Colour Atlas, Carbonate Sediments and Rocks under the Microscope*; CRC Press: Boca Raton, FL, USA, 1998; p. 330.
46. Chatzigrigoriou, A.; Manoudis, P.N.; Karapanagiotis, I. Fabrication of water repellent coatings using waterborne resins for the protection of the cultural heritage. *Macromol. Symp.* **2013**, *331*, 158–165. [CrossRef]
47. Zornoza-Indart, A.; Paula Lopez-Arce, P. Silica nanoparticles (SiO_2): Influence of relative humidity in stone consolidation. *J. Cult. Herit.* **2016**, *18*, 258–270. [CrossRef]
48. Adamopoulos, F.G.; Vouvoudi, E.C.; Achilias, D.S.; Karapanagiotis, I. Fluorosilane Water-Repellent Coating for the Protection of Marble. *Wood Other Mater. Herit.* **2021**, *4*, 2668–2675.
49. Yao, W.; Li, Y.; Huang, X. Fluorinated poly(meth)acrylate: Synthesis and properties. *Polymers* **2014**, *55*, 6197–6211. [CrossRef]
50. Aslanidou, D.; Karapanagiotis, I.; Panayiotou, C. Tuning the wetting properties of siloxane-nanoparticle coatings to induce superhydrophobicity and superoleophobicity for stone protection. *Mater. Des.* **2016**, *108*, 736–744. [CrossRef]
51. Mosquera, M.J.; Carrascosa, L.A.M.; Badreldin, N. Producing superhydrophobic/oleophobic coatings on Cultural Heritage building materials. *Pure. Appl. Chem.* **2018**, *90*, 551–561. [CrossRef]
52. *Normal—11:85*; Assorbimento d'Acqua per Capillarità Coefficiente d'Assorbimento Capillare. Istituto Centrale del Restauro: Rome, Italy, 1986.
53. *UNI EN 1926*; Metodi di Prova per Pietre Naturali—Determinazione della Resistenza a Compressione Uniassiale. 2007.
54. *UNI EN ISO 7783*; Pitture e Vernici—Determinazione delle Proprietà di Trasmissione del Vapore Acqueo—Metodo della Capsula. ISO: Geneva, Switzerland, 2019.
55. Franzoni, E.; Fregni, A.; Gabrielli, R.; Graziani, G.; Sassoni, E. Compatibility of photocatalytic TiO_2-based finishing for renders in architectural restoration: A preliminary study. *Build. Environ.* **2014**, *80*, 125–135. [CrossRef]
56. Graziani, L.; Quagliarini, E.; Bondioli, F.; D'Orazio, M. Durability of self-cleaning TiO_2 coatings on fired clay brick façades: Effects of UV exposure and wet & dry cycles. *Build. Environ.* **2014**, *71*, 193–203.
57. Roveri, M.; Goidanich, S.; Toniolo, L. Artificial Ageing of Photocatalytic Nanocomposites for the Protection of Natural Stones. *Coatings* **2020**, *10*, 729. [CrossRef]